Vorjohann, F.; Schulz, L.; Janßen, M.; Schiffers, R. (2022) Automated optimization of a block-head-mixer with an innovativealgorithm.
In: *ANTEC 2022: Conference Proceedings of the 2022 SPE Annual Technical Conference*. SPE, Society of Plastics Engineers.

AUTOMATED OPTIMIZATION OF A BLOCK-HEAD-MIXER WITH AN INNOVATIVE ALGORITHM

Felix Vorjohann, Lucas Schulz, Mirco Janßen and Reinhard Schiffers
University of Duisburg-Essen, Institute of Product Engineering (IPE), Duisburg, Germany

Abstract

CFD-Simulations are a common tool to design and optimize mixing elements. The manual evaluation and experience-based derivation of an optimized geometry is still an iterative process which is time consuming. In this paper an automated algorithm is developed and tested for a mainly distributive Block-Head-Mixer. To automatically evaluate the flow field of each geometry variant, quality criteria are introduced which enable the assessment of the mixing capability. The investigation showed that the quality criteria are suitable to evaluate the flow field and an optimized candidate compared to a starting geometry could be found automatically.

Introduction

In polymer processing mixing elements are utilized to ensure the thermal and material homogeneity of the melt. Especially the processing of additives or masterbatches requires a uniform distribution of the disperse phase in the polymer matrix. It is increasingly common to use CFD-Simulations to investigate the mixing capability of mixing elements. Several figures were developed to evaluate the distributive and dispersive mixing capabilities. For example, the famous mixing index λ according to equation (1) describes the ratio between deforming $|\bar{\bar{D}}|$ and rotional $|\bar{\bar{W}}|$ flow properties [1]:

$$\lambda = \frac{|\bar{\bar{D}}|}{|\bar{\bar{D}}| + |\bar{\bar{W}}|} \quad (1)$$

A value of zero means that pure rotational flow is acting on the melt while a value of one means pure elongational flow.

CFD-Simulations allow a significant reduction of time-consuming experimental testing. In addition, a detailed insight into the flow mechanisms can be obtained which enables the analysis of process variables that cannot be determined in experiments. But still, the CFD-based optimization process can be evolved even further when the iterative design process is replaced by an automated algorithm. The automatization of the optimization process can replace the iterative design process where an expert decides from simulation to simulation which geometry parameters should be adjusted for the next simulation run. The need for research in this field is underlined by several projects which address the automated optimization of dynamic mixing elements. [2, 3, 4]

In this paper the algorithm, which was conceptually presented in [5], for the automated design of dynamic mixing elements will be installed and investigated. A mainly distributive Block-Head-Mixer (BHM) will be optimized. Before the geometry of BHM and the optimization itself is explained, the algorithm will be introduced in the next section.

Algorithm for Automated Optimization

The CFD-Software ANSYS Fluent ® is used to create the necessary framework for the algorithm which is displayed in Figure 1.

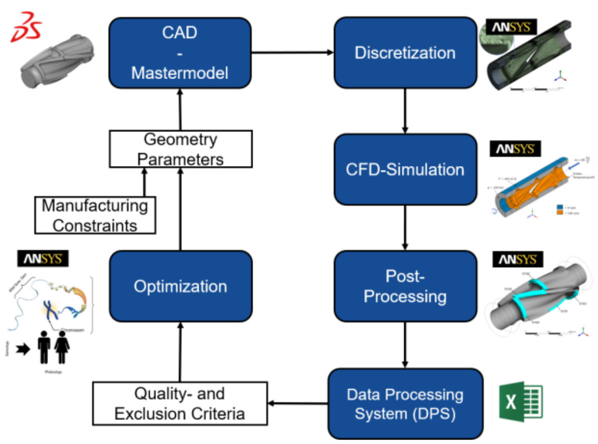

Figure 1: Algorithm for automated optimization

The blue boxes represent the main steps while the white boxes contain data which are either input or output data of the algorithm.

The algorithm was provided with a fully parameterized CAD-Mastermodel in which mixing element specific geometric degrees of freedom are defined. A range had to be determined in which the parameters can be varied, and the manufacturing constraints were considered. Then the fluid volume from the mixing element was generated and discretized in the next step.

For the discretization process global mesh settings were used to ensure that the same element sizes, growth rates and the number inflation layers were utilized for each new geometry variant. Structured prismatic layers close to the walls were necessary to consider the high velocity gradients, whereas central areas of the fluid volume were discretized with unstructured tetrahedral elements.

The discretized model was transferred to the CFD-Simulation module, in which the numerical calculation of the flow field was carried out for each variant. Each geometry variant was simulated with the same boundary conditions (rotor speed, material, mass throughput,…) so that the results could be compared among the variants. Since dynamic mixing elements create transient flow fields which require a significant simulation time, the principle of kinematic reversal was applied. This principle allowed to convert an instationary flow field to a stationary. In ANSYS, this principle was implemented using a moving reference system, so-called moving reference frames [6]. For further information on this topic, please refer to [6] and [7].

After the flow field has been calculated, the results from the solver were transferred to post-processing. Not every statistical variable could be conveniently created and analyzed in the evaluation environment. Therefore, all relevant flow parameters were exported to the data processing system (DPS) and a separate calculation was carried out with specially programmed macros before the values were returned to ANSYS. These values were quality criteria and served the optimizer as a database for determining an "optimal" candidate that met the quality criteria in the best possible way while the exclusion criteria were fulfilled. As a mathematical optimizer a genetic algorithm was utilized. Before the quality and exclusion criteria are presented in the next section, it is explicitly pointed out at this point that only those criteria were considered which allowed an assessment of a single-phase flow on a macroscopic level. Conclusions about the microscopic behavior, for example about droplet distribution, breakage, or coalescence processes as Celik did in his dissertation [8], were therefore not possible. Celik's model was applied to a fluid volume limited in size and complexity (6300 cells), whereas the algorithm presented, was designed to simulate an entire mixing element (> 1 million cells). Consequently, the computing time for the optimization is higher. In this paper, a total of eleven different quality criteria were tested and their suitability for the automated assessment of the mixing quality was examined. The user must be aware that any aggregation of information inevitably leads to a loss of information. A critical assessment of the optimization results is therefore not spared.

Quality and Exclusion Criteria

As mentioned above, eleven different quality criteria were used to evaluate the mixing quality, which will be explained in more detail below. Each individual quality criterion described an objective function that was to be minimized in the optimization. The criteria were divided into the categories *performance* and *mixing mechanisms*. The category mixing mechanisms was again divided into the sub-categories *distributive* and *dispersive*. The individual quality criteria and the assignment within the categories are listed in Table 1 below. The index of each quality criterion represented an acronym of the investigated quantity (e.g. temperature distribution = TD).

Table 1. Overview of used quality criteria

		Term	Description
Perfor-mance		QC_{FCE}	**F**luid **C**hange **E**ffectiveness
		QC_{MFR}	**M**ass **f**low **r**atio
		QC_{TRi}	**T**emperature **r**ise
Mixing Mechanisms	Distributive	QC_{TD}	**T**emperature **d**istribution
		QC_{TRa}	**T**emperature **ra**nge
		QC_{LM}	**L**ongitudinal **m**ixing
		QC_{PS}	**P**assive **s**calar
	Dispersive	QC_{LSS}	**L**ocal **s**hear **s**tress
		QC_{DSS}	**D**uration of **s**hear **s**tress
		QC_{GMI}	**G**lobal **M**ixing **I**ndex
		QC_{SD}	**S**hear **d**istribution

A normalization of the individual quality criteria to a fixed range of values was not carried out, as the criteria were subject to varying degrees of fluctuation, which were unknown in advance of the investigation. Defining a range of values for normalization without first having reliable data would have had the consequence, that individual criteria could make a meaningful comparison difficult. This would have been the case if values occured outside the expected interval or if the selected interval was too large. Instead, the quality criteria were scaled with the use of a reference geometry of the analyzed mixing element. For the reference geometry all quality criteria therefore resulted in the value one. In the evaluation, this allowed one of the following statements to be made directly based on the quality criteria of a geometry variant:

$QC < 1$: Variant is better than reference geometry
$QC = 1$: Variant is equivalent to reference geometry
$QC > 1$: Variant is worse than reference geometry

The individual criteria were combined into the aggregated criteria $QC_{Performance}$, $QC_{Distributive}$ and $QC_{Dispersive}$ using the weighted sum method. This was followed by a further aggregation to the final criterion QC_{FINAL}, which was to be minimized during the optimization.

In this paper, only a selection of the used quality criteria will be explained in detail, because an in-depth description of all criteria would exceed the scope of the paper. The other criteria were evaluated using standard methods of descriptive statistics, for example on the outlet plane of the geometry. The performance criteria included such criteria that evaluate process-related parameters such as a uniform mass flow, temperature rise and purging of the element. The latter was made assessable by the so-called fluid change effectiveness (FCE) which was adapted by Kummerow and Wortberg [9] for polymer flows based on a concept developed by Spalding [10]. The fluid change effectiveness ε is mathematically described by the following equation, where τ is the mean residence time and θ is the local mean age of the melt.

$$\varepsilon = \frac{\tau}{\theta} \tag{2}$$

For a given value of $\varepsilon = 0.5$ a quality criterion Q_{ε} could be formulated which relates the volume of all cells with $\varepsilon \leq 0.5$ to the total fluid volume. For this study, the criterion presented by [9] was related to the reference geometry according to (3) to obtain the criterion QC_{FCE} where j is the index of each geometry variant under consideration.

$$QC_{FCE,j} = \frac{Q_{\varepsilon,j}}{Q_{\varepsilon,reference}} \tag{3}$$

From the distributive criteria, the criterion QC_{PS} shall be described. It allowed the evaluation of the distributive mixing potential by including a passive scalar based on an additional transport equation which was solved during the simulation. A similar approach has been used by Hopmann et al. [11]. At the inlet, half of the area was assigned the value one, whereas the other half was assigned with the value zero. This allowed the evaluation of the distribution of the scalar transported through the fluid volume by the convective flow. A value of 0.5 at the outlet of the system would correspond to perfect distributive mixing. To calculate the criterion QC_{PS}, the mean absolute deviation of the mass flow weighted scalar at the outlet of each geometry variant $\delta_{PS(\dot{m}),j}$ is set in relation to the value of the reference (4).

$$QC_{PS,j} = \frac{\delta_{PS(\dot{m}),j}}{\delta_{PS(\dot{m}),reference}} \tag{4}$$

The criteria from the last group evaluate the dispersive mixing potential. Next to the mixing index, already described in the introduction, local shear stresses QC_{LSS} were evaluated. In this context, local means, that the points in the mixing element, where the highest shear rates were expected, were examined. For the BHM, this was in the area of the blocks. The calculation for the criterion QC_{LSS} was performed using the mean shear rates of the local volume $\mu_{\dot{\gamma}(V_{local}),j}$ (Figure 4). According to (5) this value is set in relation to the value of the reference.

$$QC_{LSS,j} = \frac{\mu_{\dot{\gamma}(V_{local}),reference}}{\mu_{\dot{\gamma}(V_{local}),j}} \tag{5}$$

In addition to the quality criteria, three different exclusion criteria were considered. They ensure that certain limits of process-related and numerical values were not exceeded. The first one limits the pressure loss to a fixed value that had to be set according to the used extrusion hardware. The second one refered to the discretization process and was intended to ensure that only those geometry variants were included in the evaluation for which sufficient mesh quality (element skewness < 0.94) was guaranteed. The last one limits the number of allowed elements for the discretization, to reduce simulation time. There was a risk that the optimal variant was not considered due to the exclusion criteria. For this reason, it had to be checked which variants were excluded and decided whether the exclusion was reasonable regarding mixing potential.

Investigation of the Algorithm

In the following section, the algorithm based on the evaluation of quality criteria is investigated. First, the initial geometry is presented and then the simulation setup and the evaluation of the results are discussed.

Geometry

A Block-Head-Mixer, based on the work of Marschik et al. [12, 13], was used as test geometry for the investigation of the optimization algorithm. Preliminary studies confirmed a great accordance of the used geometry and simulation model in this work, compared to the results of Marschik et al. [12, 13]. In Figure 2 the structure (top) and a half section of the unwounded surface (buttom) of the BHM is displayed. The parameters varied during the optimization are marked with an asterisk.

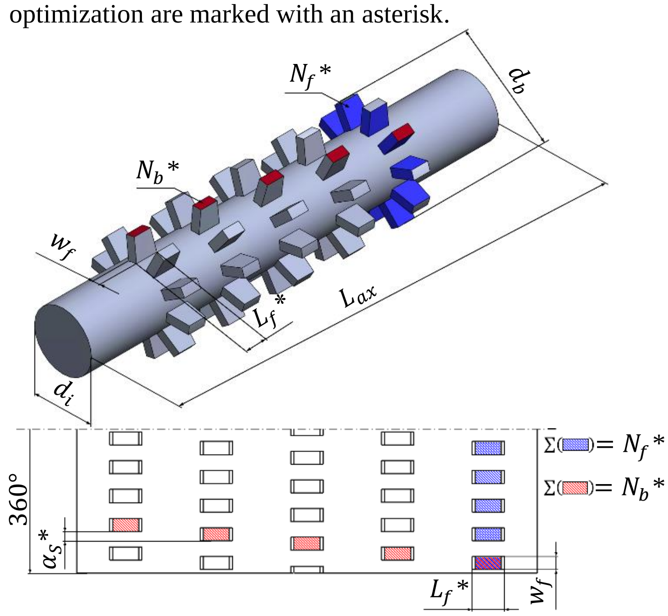

Figure 2. Geometric structure and relevant parameters of the BHM

The parameter N_f indicated the number of flights located in a block. The flights were arranged radially on the shaft. N_b described the number of blocks. The parameter α_S corresponded to the stagger angle between two successive blocks and L_f corresponded to the length of a single flight in axial direction. The remaining parameters described the width of a flight ($w_f = 4\,mm$), the root diameter of the shaft ($d_i = 28\,mm$), the barrel diameter ($d_b = 48\,mm$) and the length of the mixing element ($L_{ax} = 180\,mm$).

The varied geometry parameters and their ranges of change as well as the used step sizes are listed in Table 2. The step sizes of the parameters N_f, N_b and α_S corresponded to the work of Marschik et al. [12]. Additionally, the parameter L_f was also included in the optimization. The maximum ensured that flights of two different blocks could not collide with each other.

Table 2. Geometry parameters of the BHM

Term	Description	Reference geometry	min	max	Step size
N_f	number of flights	10	6	12	2
N_b	number of blocks	4	4	7	1
α_S	stagger angle	0°	0°	18°	6°
L_f	axial flight length	10 mm	4 mm	14 mm	2 mm

The values of the geometry parameters were varied between minimum and maximum during optimization in order to achieve an improvement of the mixing quality.

Simulation-Setup

The material used was a low-density polyethylene (PE-LD) named *Lupolen2420D* from LyondellBasell. The material properties of density, specific heat capacity, thermal conductivity and viscosity of the fluid were imported into the solver. For the properties of the solid material adjacent to the fluid, the stored values for steel in ANSYS Fluent were used. Further boundary conditions are visualized in Figure 3.

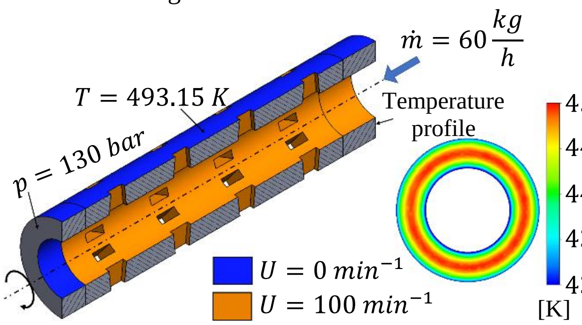

Figure 3. Boundary conditions for the simulation

A mass flow of $60\,kg/h$ and a temperature profile were set at the inlet. At the outlet, a pressure of $130\,bar$ was defined. A temperature of $220\,°C$ was set on the walls in contact with the barrel, and the boundary surfaces in contact with the shaft were treated adiabatically. To simulate the rotation speed of the BHM a moving reference frame approach was utilized so that the dynamic problem could be modeled as a steady-state problem with respect to the moving frame [6].

Simulation-Evaluation

The evaluation was performed in ANSYS CFD-Post and focused on the calculation of the quality criteria presented above. Calculations were carried out on control surfaces and volumes, which are presented in the following. Figure 4 shows the used planes for the evaluation as well as an isovolume (V_{local}) used for the evaluation of the shear stress.

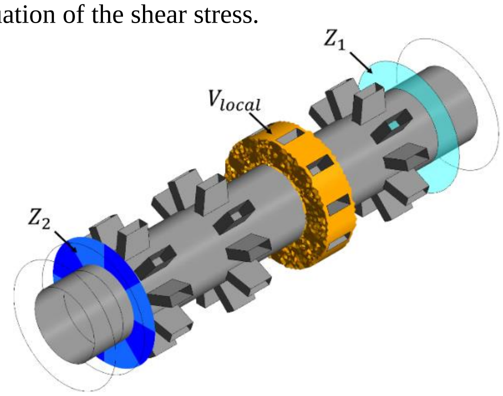

Figure 4. Evaluation planes and isovolume in ANSYS CFD-Post

For each geometry, the isovolume was located in the second block. The dimensions of the isovolume were variable in a way that the spatial extension in z-direction corresponded to the axial flight length. Also, the duration of the shear stress was evaluated using this volume. The plane Z_2 was divided into the blue shaded subplanes. These were used to determine the ratio of the mass flow for the criterion QC_{MFR}. The evaluation of the global mixing index was done via an isovolume, which was located between the planes Z_1 and Z_2 (it is not included in Figure 4).

Results of Optimization

In this section, a closer look on the results of the optimization is taken. To compare the geometry-determining parameters of the reference and the optimal candidate, Table 3 gives an overview of the results.

Table 3. Geometry parameters of reference geometry and optimal candidate

Parameter	Reference geometry	Optimal Candidate
N_f	10	6
N_b	4	6
α_s	0°	6°
L_f	$10\,mm$	$10\,mm$

Compared to the reference geometry, the number of flights per block was reduced to six, which corresponded to the defined minimum. The number of blocks increased to six and the angular offset between the flights on different blocks was 6° in the optimum geometry. The axial flight length remained unchanged and was $10\,mm$ in the optimum. In Figure 5, the reference geometry and the optimum geometry are displayed.

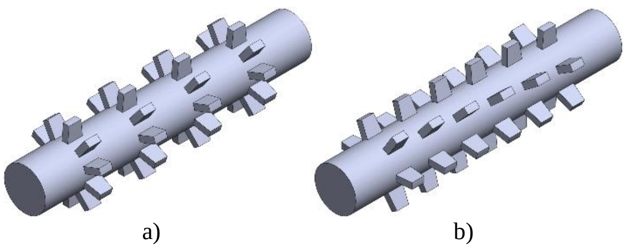

Figure 5. a) reference geometry and b) optimal candidate

To investigate the change in the final criterion, as well as the aggregated and the single criteria compared to the reference, the following Figure 6 shows all values of the calculated quality criteria of the optimal candidate.

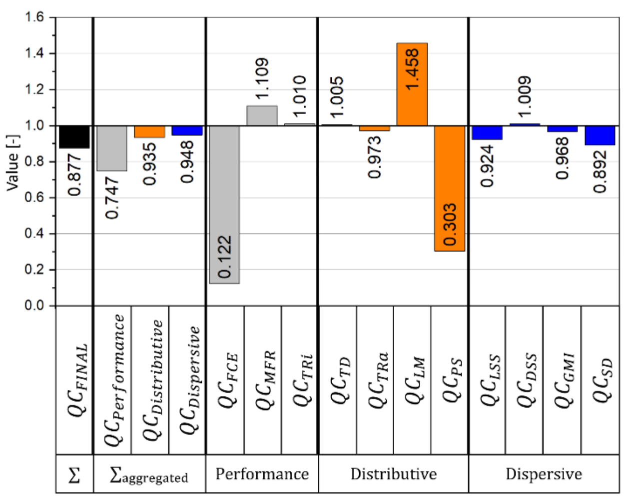

Figure 6. Quality criteria for the optimum geometry

The performance criteria are shown in gray, the distributive ones in orange, and the dispersive quality criteria in blue. The final criterion is shown in black. The value of one was chosen as the starting point of the bars in order to be able to show the direct comparison with the reference geometry for all individual and aggregated criteria. A shift of the bar upwards describes a regression of the considered criterion, while a shift downwards represents an improvement compared to the reference. As it can be seen most criteria show improvements. Especially the aggregated performance criterion was influenced by QC_{FCE} which was significantly reduced to 0.122. The distributive criterion QC_{PS} could also be considerably reduced to 0.303. The final criterion QC_{FINAL} improved to a value of 0.877.

Since the quality criteria of the optimum geometry were relative values with respect to the reference geometry, the optimum exhibited a strong dependence on the reference. This dependence has a particularly strong effect if the reference geometry itself has extreme values for one or more quality criteria. To avoid an unfavorable choice of the reference geometry, it is recommended to carry out a preliminary design based on experience or analytical formulas. In that way only appropriate technical ranges for the parameter change are considered in the simulation.

In the following, the influence of the geometry parameters on the quality criteria QC_{FINAL} is investigated. For this purpose, QC_{FINAL} was considered as a function of the two geometry parameters N_f and L_f which were identified as major influencing parameters. For a better visualization, all values of QC_{FINAL} from each geometry variant were grouped to their geometry parameter value of N_f or L_f. Mean values were formed from the grouped values, which were then used to visualize a potential trend. The trend line and the grouped values of QC_{FINAL} are displayed in Figure 7 for the number of flights N_f and the axial flight length L_f.

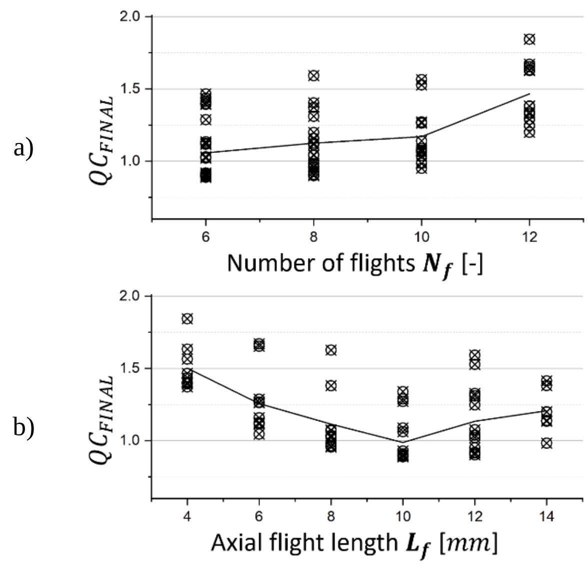

Figure 7. Influence of a) number of flights N_f and b) axial flight length L_f on the final criterion QC_{FINAL}

The data implies that lower values for N_f led to a higher mixing quality. This consideration was supported by the optimum geometry, which possessed the minimum number of flights $N_f = 6$. The strongest influence on the result of the optimization as exerted by the axial flight length L_f. There was a noticeable optimum for an axial flight length between $8\,mm$ and $12\,mm$, as shown in Figure 7. The optimum geometry also showed an axial flight length of $10\,mm$.

The number of blocks N_b exerted a weak influence on the mixing quality, no clear trend could be identified. The smallest influence on the result of the optimization was caused by the stagger angle α_S, no significant trend could be seen here. This matches the results of Marschik et al. [12], where α_S was also found to be of minor significance.

Conclusions & Outlook

In this paper, an algorithm for the automated optimization has been successfully developed and implemented. The algorithm was tested on a Block-Head-Mixer. Four geometry-defining parameters were varied and their effect on a final criterion was analyzed. The final criterion indicates the mixing capability of the flow field as well as the performance of the mixer. An optimal candidate could be determined which was able to realize a higher simulated mixing potential than the reference geometry. From the investigated parameters the axial flight length proved to have the strongest impact on the mixing potential. These results must be validated in future studies by experimental testing.

As the optimal geometry reached the defined minimum for the number of flights, future studies of the presented algorithm could cover a wider range for this parameter. The identified optimum geometry can be further verified by changing the used reference geometry and thus running the optimization from a different starting point.

The time saved during the optimization process using the automated algorithm compared to an iterative optimization cannot be stated exactly. While the fully automated generating and evaluation of every geometry saves time compared to an iterative approach, another advantage of the automated algorithm is the independence of the resulting geometry from the personal experience of the operating engineer.

References

1. J.-F. Agassant, I. Manas-Zloczower, *Mixing and compounding of polymers. Theory and practice*, Hanser, München, 2009.
2. S. Hube, M. Behr, S. Elgeti, M. Schön, J. Sasse, C. Hopmann, *Numerical Design of Distributive Mixing Elements*, Cornell University, 2021.
3. S. Elgeti, C. Hopmann, *Automatisierte Auslegung und Optimierung von dynamischen Misch- und Scherteilen für Einschneckenextruder*, Project outline, Institute for Plastics Processing, RWTH Aachen University, Germany.
4. C. Bonten, *Analyse dispersiver Mischprozesse in Kunststoffschmelzen, Project outline, Institut für Kunststofftechnik*, University of Stuttgart, Germany, https://gepris.dfg.de/gepris/projekt/285787361.
5. M. Janßen, R. Schiffers, *Design of a Novel Free-Rotating Mixing Sleeve for Single-Screw Extrusion*, in Proceedings of SPE ANTEC Conference, San Antonio (Texas), USA, 2020.
6. ANSYS, *Fluent User's Guide 2019.*
7. G. A. Campbell, M.A. Spalding, *Analyzing and troubleshooting single-screw extruders*, Hanser, München, 2013.
8. O. Celik, *Neuartiges Simulationsmodell zur Vorhersage der prozessinduzierten Morphologieausbildung in heterogenen Kunststoffblends*, Dissertation, Universität Stuttgart, Stuttgart, 2018.
9. J. Kummerow, J. Wortberg, *Local mean age of melt: New approaches for die optimization,* Proceedings of PPS-34: the 34th International Conference of the Polymer Processing Society (PPS), Taipei, Taiwan, 2019.
10. D. B. Spalding, *A note on mean residence-times in steady flows of arbitrary complexity,* in: *Chemical Engineering Science* 9 (1), S. 74–77, 1958.
11. C. Hopmann, M. Schön, M. Reul, M. Facklam, *A Method for the Validation of Simulated Mixing Characteristics of Two Dynamic Mixers in Single-Screw Extrusion,* in Poylmers 12, 2020.
12. C. Marschik, T. Osswald, W. Roland, H. Albrecht, O. Skrabala, J. Miethlinger, *Numerical analysis of mixing in block-head mixing screws,* in: Polymer Engineering & Science 59 (s2), E88-E104. DOI: 10.1002/pen.24968, 2019.
13. C. Marschik, *Functional Process Analysis of Single-Screw Extrusion. Modeling Melt Conveying*, Devolatilization, and Mixing. Dissertation, Linz, 2018.

DOI: 10.17185/duepublico/79222
URN: urn:nbn:de:hbz:465-20231026-152052-7

Vorjohann, F.; Schulz, L.; Janßen, M.; Schiffers, R. (2022) Automated optimization of a block-head-mixer with an innovative algorithm. In: *ANTEC 2022: Conference Proceedings of the 2022 SPE Annual Technical Conference*. SPE, Society of Plastics Engineers. https://www.4spe.org